Electronic Supplementary Information

MLCC fabrication

The produced 0.8BFBT-0.2NT ceramic powders were added with polyvinyl butyral (PVB) binde, water-free alcohol, and B76 solution. Using 3 mm-diameter ZrO_2 balls and dispersant, powders with PVB binder were mixed in a conventional ball mill for 8 h. Then, di(2-ethylhexyl) phthalate (DEHP) plasticizer was added and mixed again for another 18-h ball milling process to obtain the ceramic slurry. Tape casting method was employed to fabricate ceramic layers. The ceramic slurry was poured into the tape casting machine with a thickness of ~25 μm. The produced ceramic tape was cut into rectangular shapes with a dimension of 5 cm×7 cm. The rectangular ceramic tapes were stacked to prepare the top and bottom ceramic cover layers, followed by a hot-pressing process using 500 psi and water pressing process at 100 psi to ensure that each ceramic layer adheres to each other. The hot pressing was executed using a ~60-70 ^oC hot plate, while the water pressing was executed by placing the stacked ceramics in vacuum-sealed plastic and burying them in a water-filled chamber. The Ag/Pd (90:10) paste was screen-printed for the interfacial electrode. Every round of electrode printing was followed by ceramic tape stacking and hot pressing. After printing the last electrode layer, the top ceramic cover layer was stacked, hot pressed, printed with green dye to guide the slicing process that follows after, and water pressed. Finally, the stacked ceramics were sliced into discs of 3.4 mm×1.2 mm and sintered at 915 ^oC for 1-layer and at 930 ^oC for 9-layer and 24-layer MLCCs. The as-sintered stacked ceramics were polished, coated with top and bottom Ag electrodes (or outer electrodes), and annealed at 800 ^oC to produce the MLCCs.

Methods of analyses

A scanning electron microscope (SEM, JEOLJSM-7610F plus) was used to image the cross-section grain morphologies. A Bruker X-ray diffractometer (D8 ADVANCE ECO) was employed to investigate the lattice structures assisted by the Rietveld refinement analyses using the HighScore Plus software version 3.0.5. A HORIBA LabRAM HR Evolution system was used with a 532 nm-laser to acquire Raman scattering spectra. The nanoscale morphology and electron diffraction were probed by a 200 kV-capable transmission electron microscope (JEOL JEM-2100 LaB_6). The high-angle annular dark-field (HAADF) imaging was sided using a field-emission scanning transmission electron microscope (Thermo Fisher Scientific, Talos F200XG2) to probe the ion distribution. Using the Workstation 2000 (Radiant Technologies Precision LC II), the polarization vs. *E* field (P-E) hysteresis loops were acquired at 10 Hz frequency. The phase impedance analyzer (Wayne-Kerr PMA6420A) was used to assess dielectric permittivity and loss as functions of temperature and operation frequency. The nanoscale morphology and electron diffraction were investigated by a JEOL transmission electron microscope (JEM-2100 LaB_6) with a 200 kV-acceleration capability. The phase impedance analyzer (Wayne-Kerr PMA6420A) was used to assess dielectric properties. The electrical potential distribution on the gain matrix was probed employing a Kelvin probe force microscope (KPFM, Bruker Multimode 8).

Table S1 Energy-storage performance of various MLCCs where *N* is the active ceramic layers and *t* is the thickness of ceramic layers.

Ceramic layer	Internal electrode	*N*	*T* (*μm*)	W_{rec} ($J\ cm^{-3}$)	E_b ($kV\ m^{-1}$)	η (%)	ρ ($J\ kV^{-1}\ cm^{-2}$)	Maximum operating temperature (°C)	Reference
BT-BZT	Pt/Au/Pd	30	29	2.8	330	-	8.4×10^{-3}	-	[42]
BT-BNT	Ag/Pd	10	30	2.76	450	84.3	6.1×10^{-3}	175	[43]
BT-BZNT	Ag/Pd	10	11	8.13	750	95	10.8×10^{-3}	170	[44]
BT-BZNT-SiO_2	Ag/Pd	2	4.7	18.24	1755	94.5	10.4×10^{-3}	190	[51]
BT-BF	Ag/Pd	6	~7	20.8	1100	97.5	18.9×10^{-3}	100	[6]
BT-BLT	Pt	13	30	4.05	466	95.5	8.7×10^{-3}	160	[45]
BT-BLN	Pt	13	30	4.5	450	91.5	10×10^{-3}	160	[46]
BT-BMN	Pt	9	9	6.88	820	90	8.4×10^{-3}	85	[47]
BNF-BT	Pt	9	32	6.74	540	77	12.4×10^{-3}	125	[48]
BF-BT-NZZ	Pt	7	16	10.5	700	87	15×10^{-3}	150	[49]
NBT-0.35SBT	Pt	10	20	21.5	1000	80	21.5×10^{-3}	150	[14]
NBT-0.35SBT	Pt	10	20	9.5	720	92	13.2×10^{-3}	120	[50]
BF-BT-0.2NT	Ag/Pd	9	18	2.8	400	73	7×10^{-3}	-	This work
BF-BT-0.2NT	Ag/Pd	24	18.2	4.5	450	77	1×10^{-2}	180	This work

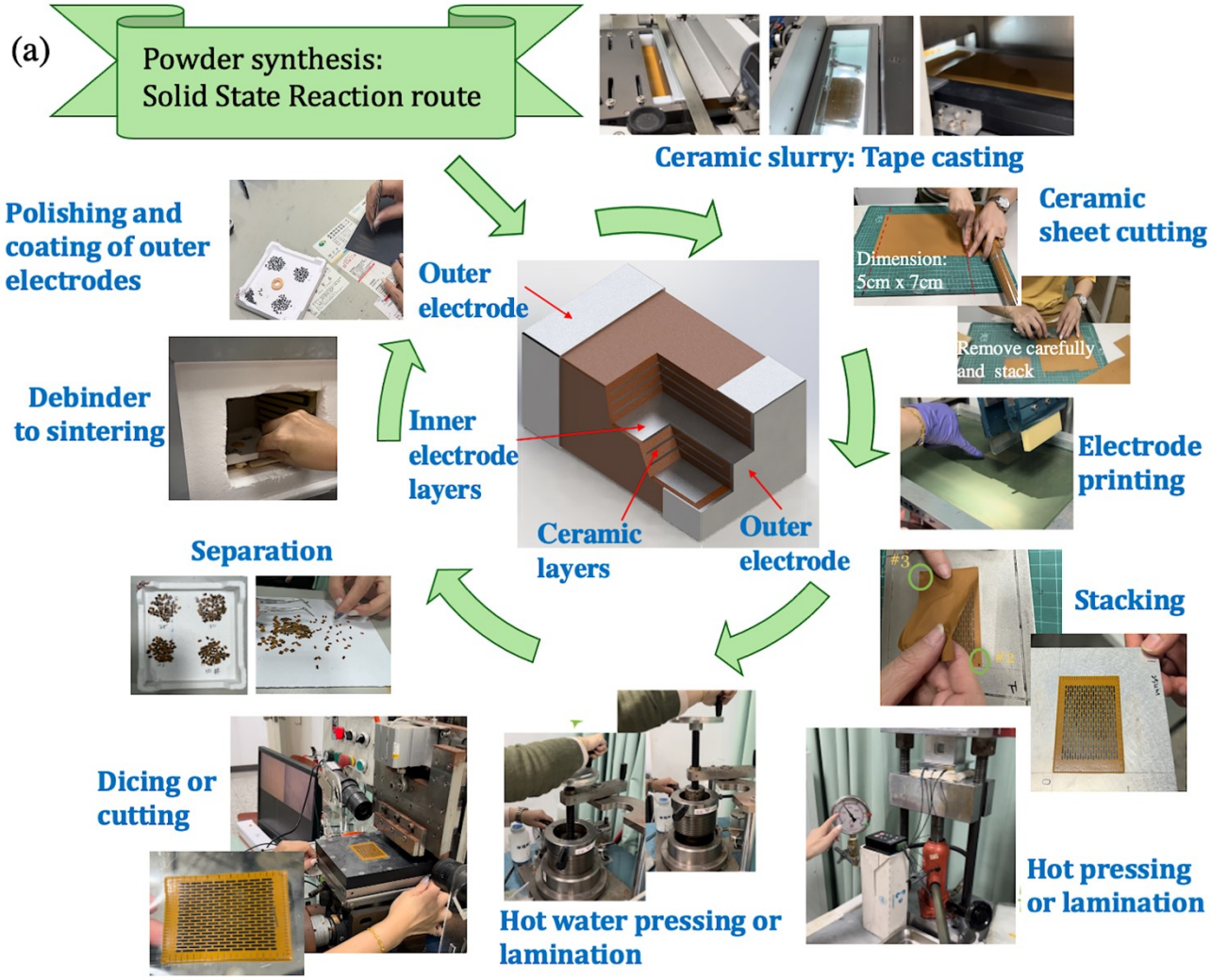

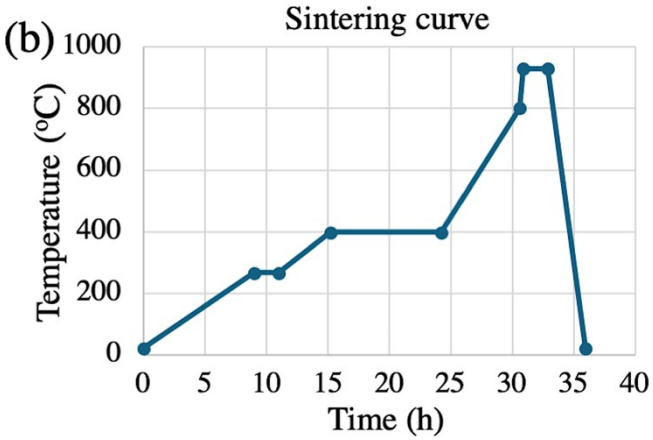

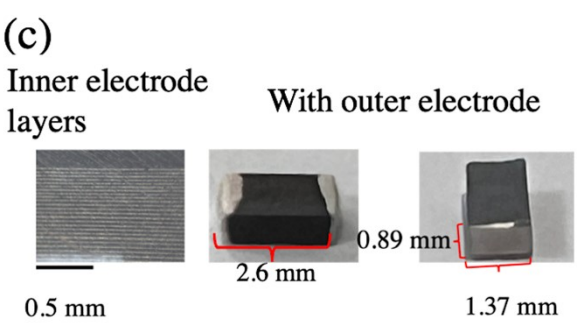

Figure S1 (a) The flow chart of the MLCC fabrication process. (b) Sintering curve of MLCC chips. (c) Actual fabricated MLCC chip and dimensions.

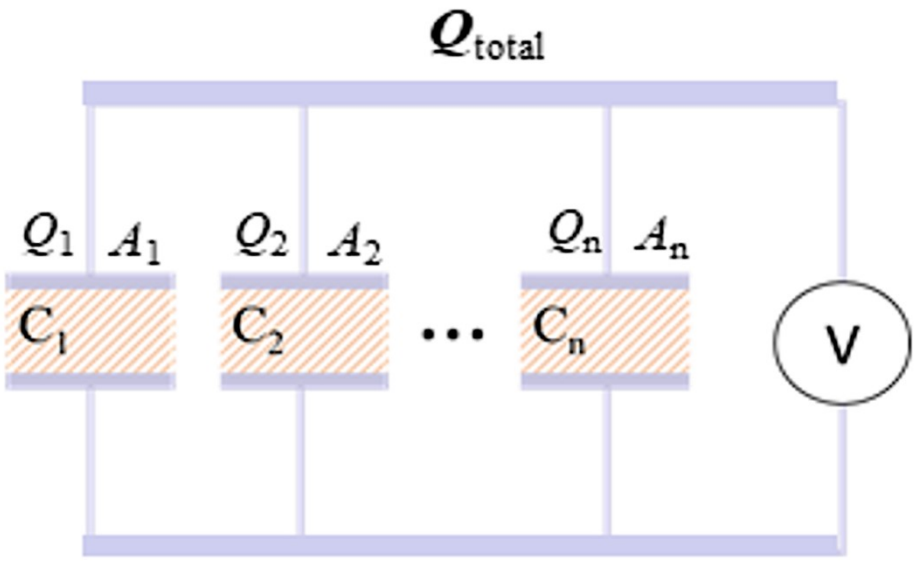

Figure S2 Equivalent capacitance in parallel-circuit MLCC design.

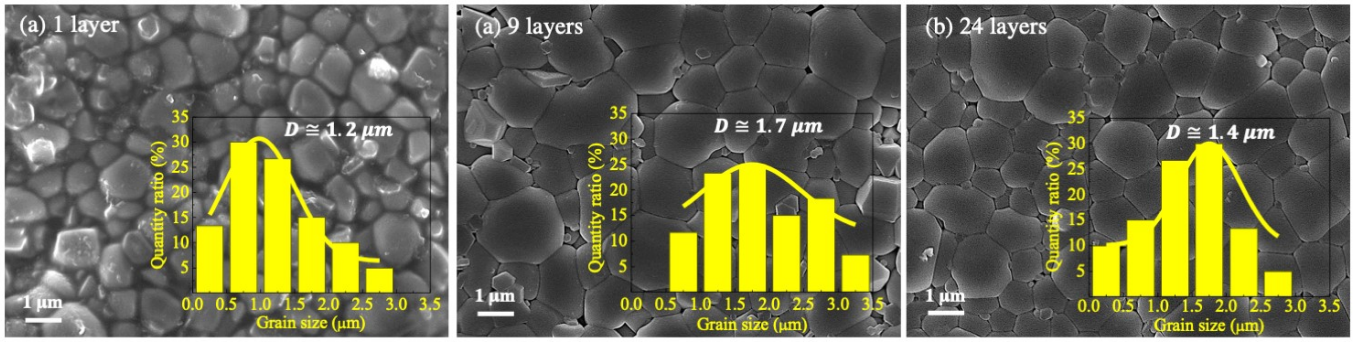

Figure S3 SEM cross-section morphologies and grain size distributions of 1-layer, 9-layer, and 24-layer MLCCs.

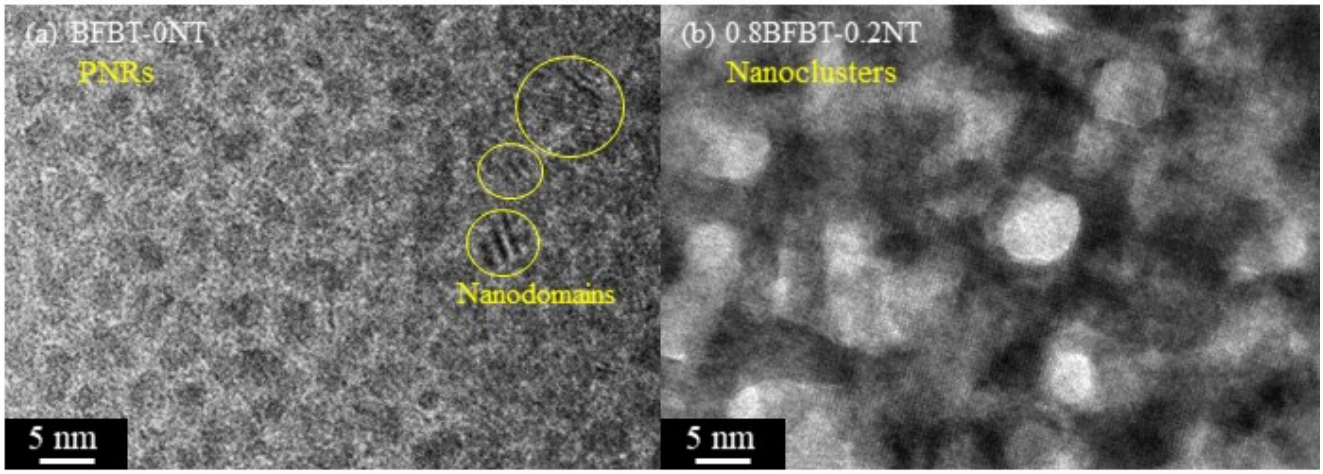

Figure S4 High-resolution TEM images of (a) BFBT-0NT and (b) 0.8BFBT-0.2NT.

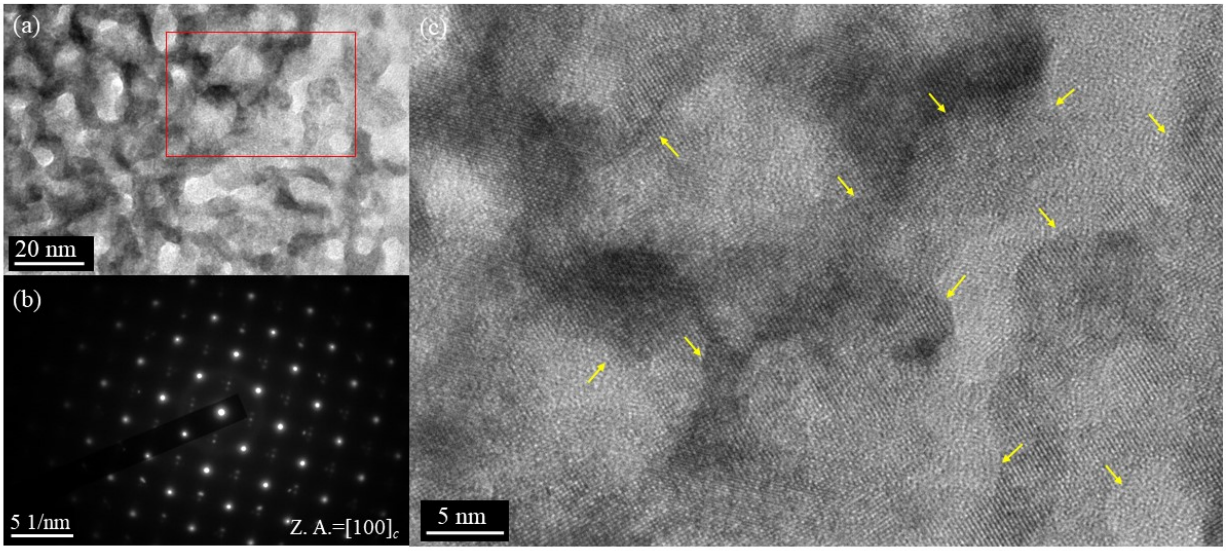

Figure S5 (a) TEM image of local nanoclusters (b) corresponding [100]-zoned SAED pattern in 0.8BFBT-0.2NT grain. (c) High-resolution TEM image enlarged from the red rectangular- box area in (a).

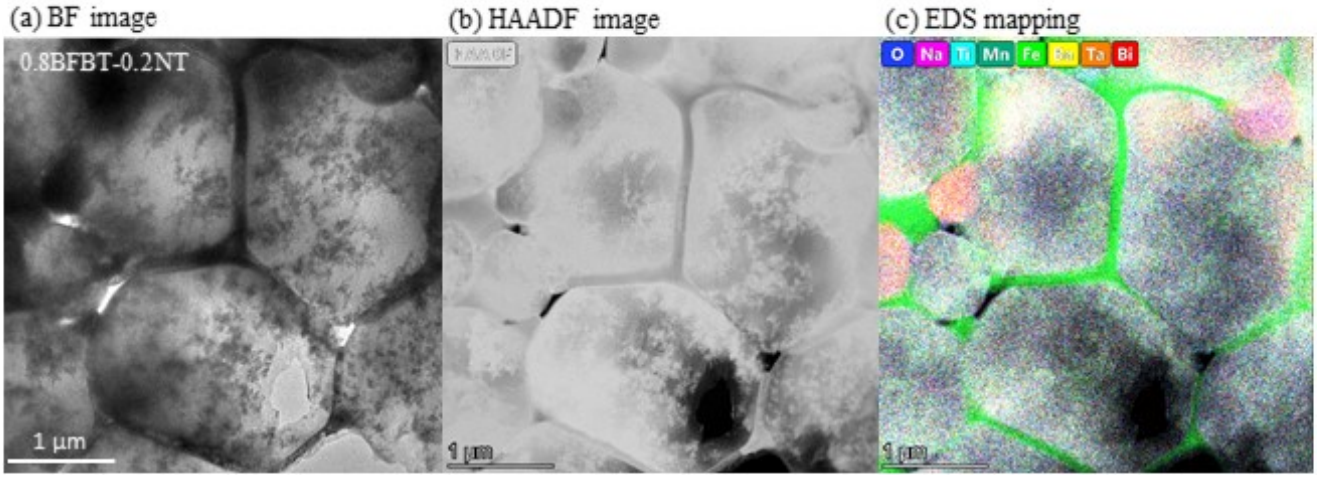

Figure S6 (a) TEM BF images, (b) HAADF image, and (c) EDS mapping of 0.8BFBT-0.2NT ceramic.

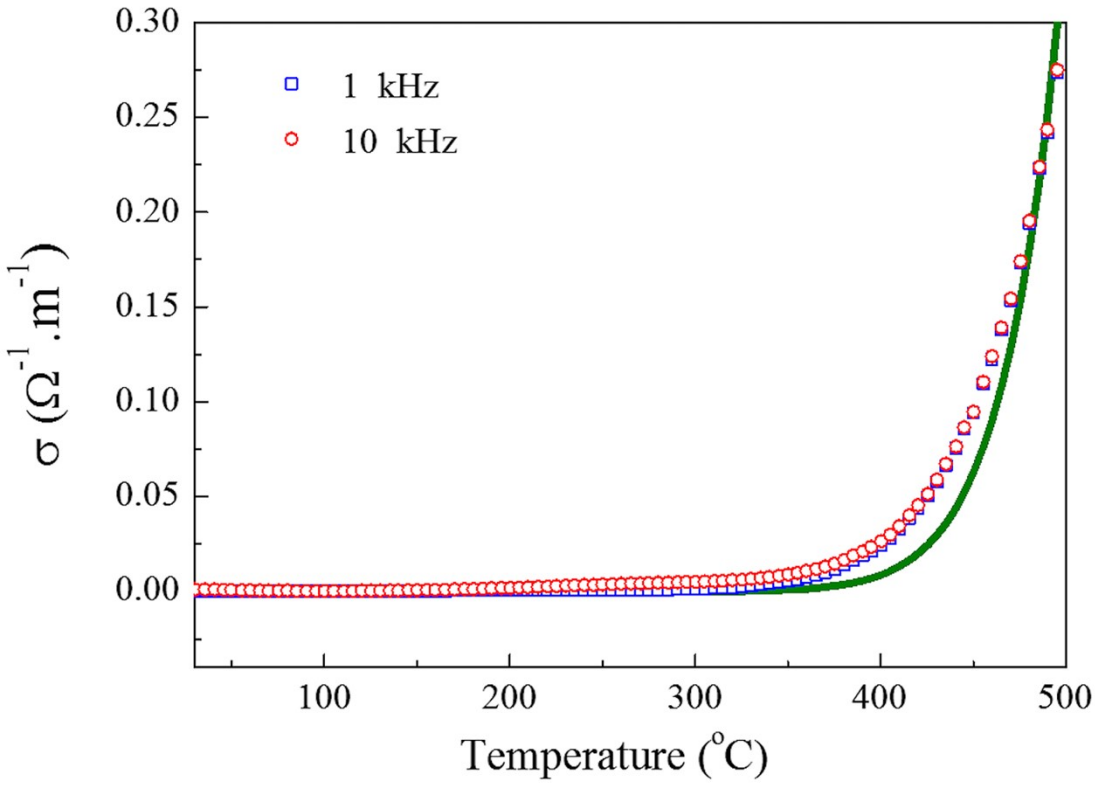

Figure S7 Conductivity ($\sigma = 2\pi f \varepsilon_o \varepsilon''$) vs temperature at 1 kHz and 10 kHz. The solid line is the fit of the relation, $\sigma = \sigma_o e^{-Ea/T}$ with σ_o =2.12×10^{10} Ω^{-1} m^{-1} and E_a = 19200 K (or 4.8×10^2 eV).